



www.sciencemag.org/cgi/content/full/science.aaa4170/DC1

Supplementary Materials for

Quantum versus classical annealing of Ising spin glasses

Bettina Heim, Troels F. Rønnow, Sergei V. Isakov, Matthias Troyer*

*Corresponding author. E-mail: troyer@phys.ethz.ch

Published 12 March 2015 on *Science Express*
DOI: 10.1126/science.aaa4170

This PDF file includes:

Materials and Methods
Figs. S1 to S4
Full Reference List

Methods

Simulated classical Annealing

Simulated annealing is performed using a single spin flip Metropolis algorithm. In Fig. S1, we linearly decreased the temperature from $T = 3$ to zero as a function of time as done in Ref. (19). This schedule produces very similar results as a linear increase of the inverse temperature from $\beta = 1/3$ to $\beta = 10$ and we use this second schedule for all other results.

Simulated quantum Annealing

To perform simulated quantum annealing by path integral quantum Monte Carlo (QMC) simulations we split the inverse temperature $\beta = 1/k_B T$ into M “imaginary time” steps $\Delta\tau = \beta/M$ and apply a Trotter-Suzuki decomposition (31, 32) to the thermal density matrix $\exp(-\beta H_q) = \exp(-\Delta\tau \cdot H_q)^M$. This results in a mapping of the partition function of the quantum system to that of a classical system consisting of a stack of M replicas of the original system. Each of these replicas corresponds to one imaginary time step in DT-SQA. Within each replica the spins are coupled by renormalized Ising couplings J_{ij}/M and the transverse field gives rise to an additional “time-like” Ising coupling of strength $J_\tau = -1/(2\beta) \cdot \log \tanh(\Gamma\Delta\tau)$ between spins in adjacent replicas.

Thermal equilibrium properties of the quantum system can be sampled by simulating this equivalent classical system, and SQA can be performed by varying the transverse field strength $\Gamma(t)$, which changes the coupling between time slices. In our simulations, the transverse field Γ is decreased linearly from $\Gamma(0) = 2.5$ to zero. The time discretization error vanishes at the end of the annealing schedule when the transverse field is switched off and all remaining terms in the Hamiltonian commute.

Segment updates: In both DT-SQA and CT-SQA we perform cluster flips of segments in imaginary time for better efficiency and use periodic boundary conditions in all directions. For any finite temperature, the probability to form clusters of length τ in CT-SQA is simply given by taking the limit $M \rightarrow \infty$ of the probability to form $\tau \cdot M$ bonds along the imaginary time axis in DT-SQA. The times τ which divide adjacent clusters of the same spin orientation, can thus be generated directly according to the exponential distribution $f(\tau) = \beta\Gamma \cdot \exp(-\beta\Gamma\tau)$.

Reproducing the results of Ref. (19): Fig. S1 shows our reproduction of the results of Ref.(19). The initial state for DT-SQA in Ref. (19) has been prepared by precooling: Initializing a classical system with a random configuration, SA is used to thermalize the system at a temperature $1/\beta$. For this thermalization, we decrease the temperature linearly from $T^{(\text{pre})} = 3$ to $1/\beta$ using 100 Monte Carlo steps (MCS). Prior to starting the simulated quantum annealing process, each replica is then initialized with the state of the thermalized classical system. Comparing the DT-SQA curves with and without precooling (see Fig. S1B), we find that precooling only results in constant offset but does not improve the scaling. We thus omit precooling from our simulations.

SQA as Classical Optimizer versus a physics simulation: There are a few crucial differences in running SQA as a physics simulation or a classical optimization algorithm, which we summarize here for completeness. Firstly, when using SQA as a classical optimizer we can tune the number of time slices M to optimize the performance, while as a physics simulation we need to take the continuous time limit. Secondly, when run as a classical optimizer we can scan all M time slices for the configuration with lowest energy, while as a physics simulation we need to either measure on just one random time slice or average over all time slices. Finally, when calculating the performance of SQA as a classical optimizer we need to multiply the annealing time as given in number of MCS by the effort for one MCS, which is proportional to the number of time slices M in DT-SQA or the extent of the imaginary time direction β in CT-SQA.

For performance reasons we used DT-SQA instead of CT-SQA when discussing properties of a physical system in Fig. 4B. We took care to choose the Trotter number M large enough for convergence to the continuous time limit. Specifically, we used 1984 Trotter slices for $\beta = 128$, 768 for $\beta = 64$, 256 for $\beta = 32$, 128 for $\beta = 16$ and 64 for all lower values of β . Our estimate on the required number of Trotter slices is based on the convergence at $M = 128$ for $\beta = 20$ shown in Fig. 3A in the main text and a scaling of the Trotter error with β^3/M^2 . A comparison between Fig. S3 and Fig. S4 shows that these estimates were indeed reasonable.

Implementation details: In order to make an efficient implementation of DT-SQA, we use individual bits in integer variables for storing the spins. Bit manipulations can then be used to build and update clusters along imaginary time. For each spin, we build clusters by using the algorithm in Ref. (33) to break segments of the same spin orientation into smaller pieces. At the beginning of the schedule, all Trotter slices are weakly coupled and only very small clusters are present. As the cluster size only increases significantly late during our schedule, using forward computation of the energies – saving and updating local energies – throughout the algorithm increases its performance. Finally, we approximate the exponential function as in Ref. (34). This approximation estimates the exponential function with a relative error up to 3.5%, but if one corrects the result using a 256-element lookup table the error can be reduced to 0.01% (and 0.001% using a 4096-element lookup table). We found that even a much large error in the calculation of the exponential would, in general, not significantly change the behavior of the algorithm.

Supplementary Data and Figures

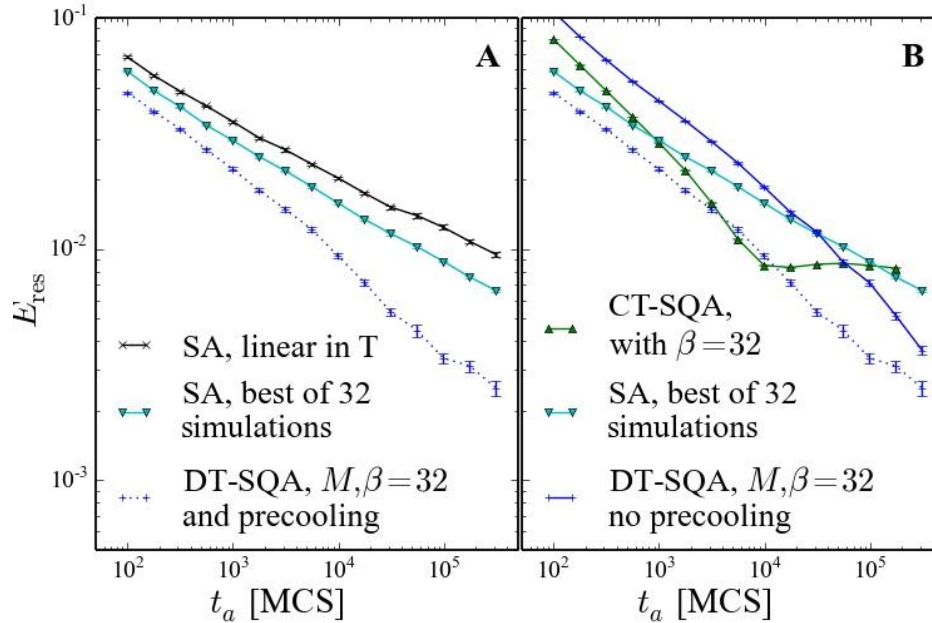


Fig. S1. Reproduction of the main result of Ref. (19).

Shown is the dependence of the residual energy E_{res} on the annealing time t_a . **A)** The residual energy E_{res} for SA, DT-SQA and **B)** CT-SQA, both for the square lattice Ising spin glass instance of Ref. (19) with 6400 spins. The annealing time t_a is in units of Monte Carlo steps (MCS), corresponding to one attempted update per spin. E_{res} and error bars are obtained by averaging over forty annealing runs. For SA, the best results of 32 independent simulations are shown additionally, such that the computational effort for all data in B is roughly the same.

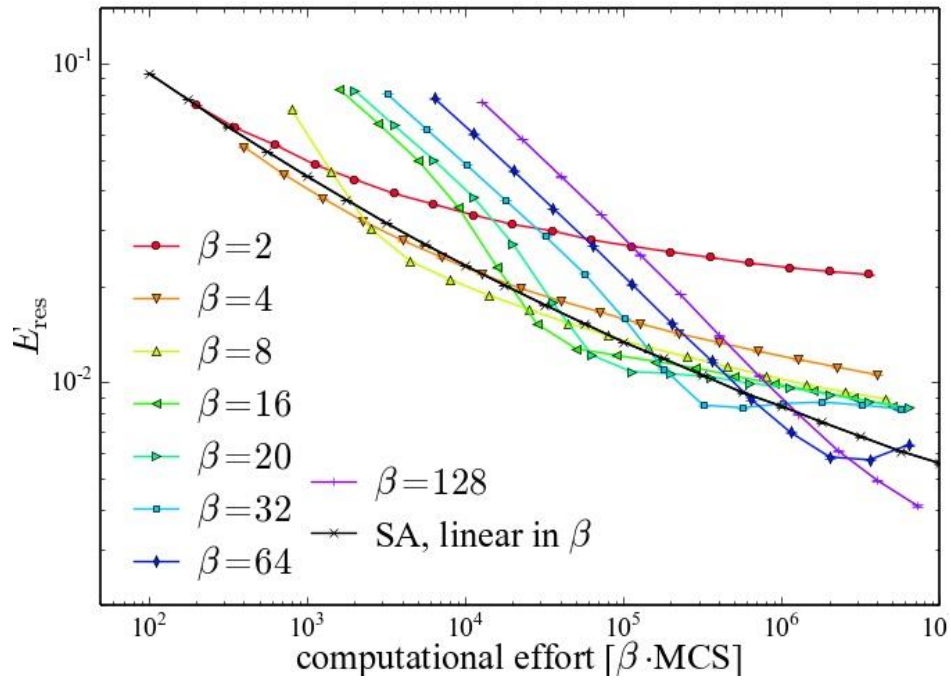


Fig. S2. CT-SQA simulations of SQA as a classical optimizer

The residual energy as a function of computational effort averaged over 1000 random disorder realizations using CT-SQA, complementing Fig. 4A in the main text. We note that, adjusting the temperature depending on the total annealing time, even CT-SQA can marginally outperform SA when used as a classical optimizer.

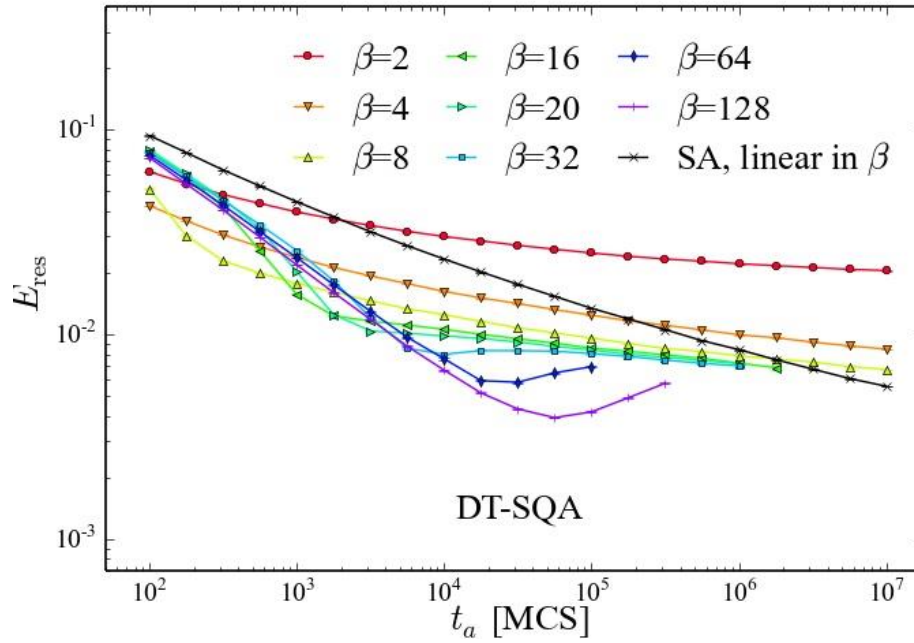


Fig. S3 Minimal residual energy over all time slices

Shown is the minimal residual energy along imaginary time, instead of averaging the residual energy shown in Fig. 4B in the main text. The same number of Trotter slices as in Fig. 4B for each value of β is used and the results are averaged over a 1000 random disorder realizations. Comparing to Fig. 4B indicates that the protocol for measuring the final energy has a significant impact on the results.

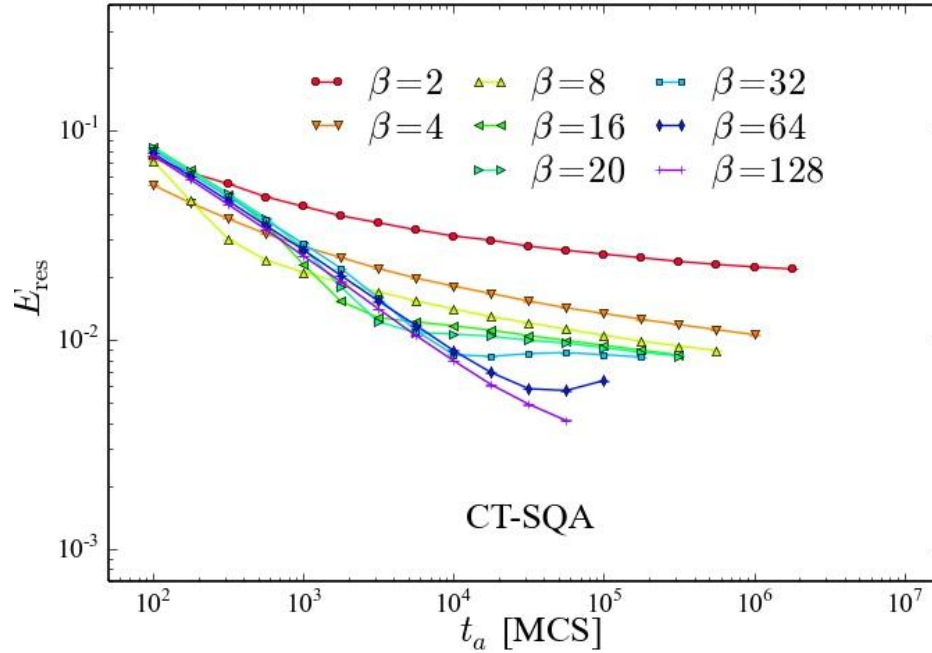


Fig. S4. Dependence of the residual energy on temperature

This figure shows the temperature dependence of the minimal residual energy with CT-SQA, complementing Fig. 3B in the main text. While we have good correspondence between CT-SQA and DT-SQA for $\beta < 20$, comparing the curves for lower temperatures, shows a slower decrease of the residual energy with annealing time for DT-SQA. The fact that by decreasing the temperature low energies can be reached also for CT-SQA is encouraging for a potential limited speedup (23) of SQA over SA in the zero-temperature limit.

References and Notes

1. M. Radivojević, T. Rehren, J. Kuzmanović-Cvetković, M. Jovanović, J. P. Northover, Tainted ores and the rise of tin bronzes in Eurasia, c. 6500 years ago. *Antiquity* **87**, 1030–1045 (2013). [doi:10.1017/S0003598X0004984X](https://doi.org/10.1017/S0003598X0004984X)
2. S. Kirkpatrick, C. D. Gelatt Jr., M. P. Vecchi, Optimization by simulated annealing. *Science* **220**, 671–680 (1983). [Medline doi:10.1126/science.220.4598.671](https://pubmed.ncbi.nlm.nih.gov/2446810/)
3. F. Barahona, On the computational complexity of Ising spin glass models. *J. Phys. Math. Gen.* **15**, 3241–3253 (1982). [doi:10.1088/0305-4470/15/10/028](https://doi.org/10.1088/0305-4470/15/10/028)
4. R. Graham, Bounds for certain multiprocessing anomalies. *Bell Syst. Tech. J.* **45**, 1563–1581 (1966). [doi:10.1002/j.1538-7305.1966.tb01709.x](https://doi.org/10.1002/j.1538-7305.1966.tb01709.x)
5. D. E. Knuth, *The Art of Computer Programming, Volume 4, Fascicle 1: Bitwise Tricks & Techniques; Binary Decision Diagrams* (Addison-Wesley Professional, 2009), 12th edn.
6. L.-P. Wong, M. Y.-H. Low, C. S. Chong, Bee colony optimization with local search for Traveling Salesman Problem. *Int. J. Artif. Intell. Tools* **19**, 305–334 (2010). [doi:10.1142/S0218213010000200](https://doi.org/10.1142/S0218213010000200)
7. S. A. Cook, in *Proceedings of the Third Annual ACM Symposium on Theory of Computing* (ACM, New York, 1971), pp. 151–158.
8. N. Metropolis, A. W. Rosenbluth, M. N. Rosenbluth, A. H. Teller, E. Teller, Equation of state calculations by fast computing machines. *J. Chem. Phys.* **21**, 1087 (1953). [doi:10.1063/1.1699114](https://doi.org/10.1063/1.1699114)
9. D. Bertsimas, J. Tsitsiklis, Simulated annealing. *Stat. Sci.* **8**, 10–15 (1993). [doi:10.1214/ss/1177011077](https://doi.org/10.1214/ss/1177011077)
10. P. Ray, B. K. Chakrabarti, A. Chakrabarti, Sherrington-Kirkpatrick model in a transverse field: Absence of replica symmetry breaking due to quantum fluctuations. *Phys. Rev. B* **39**, 11828–11832 (1989). [doi:10.1103/PhysRevB.39.11828](https://doi.org/10.1103/PhysRevB.39.11828)
11. A. B. Finnila, M. A. Gomez, C. Sebenik, C. Stenson, J. D. Doll, Quantum annealing: A new method for minimizing multidimensional functions. *Chem. Phys. Lett.* **219**, 343–348 (1994). [doi:10.1016/0009-2614\(94\)00117-0](https://doi.org/10.1016/0009-2614(94)00117-0)
12. T. Kadowaki, H. Nishimori, Quantum annealing in the transverse Ising model. *Phys. Rev. E Stat. Phys. Plasmas Fluids Relat. Interdiscip. Topics* **58**, 5355–5363 (1998). [doi:10.1103/PhysRevE.58.5355](https://doi.org/10.1103/PhysRevE.58.5355)
13. E. Farhi, J. Goldstone, S. Gutmann, J. Lapan, A. Lundgren, D. Preda, A quantum adiabatic evolution algorithm applied to random instances of an NP-complete problem. *Science* **292**, 472–475 (2001). [Medline doi:10.1126/science.1057726](https://pubmed.ncbi.nlm.nih.gov/11518613/)
14. A. Das, B. K. Chakrabarti, Colloquium: Quantum annealing and analog quantum computation. *Rev. Mod. Phys.* **80**, 1061–1081 (2008). [doi:10.1103/RevModPhys.80.1061](https://doi.org/10.1103/RevModPhys.80.1061)
15. L. Landau, *Physikalische Zeitschrift der Sowjetunion* **2**, 46 (1932).
16. C. Zener, Non-adiabatic crossing of energy levels. *Proc. R. Soc. Lond., A Contain. Pap. Math. Phys. Character* **137**, 696–702 (1932). [doi:10.1098/rspa.1932.0165](https://doi.org/10.1098/rspa.1932.0165)

17. J. Brooke, D. Bitko, T. F. Rosenbaum, G. Aeppli, Quantum annealing of a disordered magnet. *Science* **284**, 779–781 (1999). [Medline doi:10.1126/science.284.5415.779](#)
18. M. W. Johnson, M. H. Amin, S. Gildert, T. Lanting, F. Hamze, N. Dickson, R. Harris, A. J. Berkley, J. Johansson, P. Bunyk, E. M. Chapple, C. Enderud, J. P. Hilton, K. Karimi, E. Ladizinsky, N. Ladizinsky, T. Oh, I. Perminov, C. Rich, M. C. Thom, E. Tolkacheva, C. J. Truncik, S. Uchaikin, J. Wang, B. Wilson, G. Rose, Quantum annealing with manufactured spins. *Nature* **473**, 194–198 (2011). [Medline doi:10.1038/nature10012](#)
19. G. E. Santoro, R. Martonák, E. Tosatti, R. Car, Theory of quantum annealing of an Ising spin glass. *Science* **295**, 2427–2430 (2002). [Medline doi:10.1126/science.1068774](#)
20. R. Martoňák, G. E. Santoro, E. Tosatti, Quantum annealing by the path-integral Monte Carlo method: The two-dimensional random Ising model. *Phys. Rev. B* **66**, 094203 (2002). [doi:10.1103/PhysRevB.66.094203](#)
21. M. Suzuki, Relationship between d -dimensional quantal spin systems and $(d+1)$ -dimensional Ising systems: Equivalence, critical exponents and systematic approximants of the partition function and spin correlations. *Prog. Theor. Phys.* **56**, 1454–1469 (1976). [doi:10.1143/PTP.56.1454](#)
22. See the supplementary materials accompanying this paper.
23. T. F. Rønnow, Z. Wang, J. Job, S. Boixo, S. V. Isakov, D. Wecker, J. M. Martinis, D. A. Lidar, M. Troyer, Defining and detecting quantum speedup. *Science* **345**, 420–424 (2014). [Medline doi:10.1126/science.1252319](#)
24. H. Rieger, N. Kawashima, Application of a continuous time cluster algorithm to the two-dimensional random quantum Ising ferromagnet. *Eur. Phys. J. B* **9**, 233–236 (1999). [doi:10.1007/s100510050761](#)
25. www.informatik.uni-koeln.de/spinglass/.
26. S. W. Shin, G. Smith, J. A. Smolin, U. Vazirani, arXiv:1401.7087 (2014).
27. S. Boixo, T. F. Rønnow, S. V. Isakov, Z. Wang, D. Wecker, D. A. Lidar, J. M. Martinis, M. Troyer, Evidence for quantum annealing with more than one hundred qubits. *Nat. Phys.* **10**, 218–224 (2014). [doi:10.1038/nphys2900](#)
28. Y. Matsuda, H. Nishimori, H. G. Katzgraber, Ground-state statistics from annealing algorithms: Quantum versus classical approaches. *New J. Phys.* **11**, 073021 (2009). [doi:10.1088/1367-2630/11/7/073021](#)
29. E. Crosson, E. Farhi, C. Y.-Y. Lin, H.-H. Lin, P. Shor, <http://arxiv.org/abs/1401.7320> (2014).
30. H. G. Katzgraber, F. Hamze, R. S. Andrist, Glassy chimeras could be blind to quantum speedup: Designing better benchmarks for quantum annealing machines. *Physical Review X* **4**, 021008 (2014). [doi:10.1103/PhysRevX.4.021008](#)
31. H. F. Trotter, On the product of semi-groups of operators. *Proc. Am. Math. Soc.* **10**, 545 (1959). [doi:10.1090/S0002-9939-1959-0108732-6](#)
32. M. Suzuki, Generalized Trotter’s formula and systematic approximants of exponential operators and inner derivations with applications to many-body problems. *Commun. Math. Phys.* **51**, 183–190 (1976). [doi:10.1007/BF01609348](#)

33. L. Pierre, T. Giamarchi, H. Schulz, A new random-number generator for multispin Monte Carlo algorithms. *J. Stat. Phys.* **48**, 135–149 (1987). [doi:10.1007/BF01010404](https://doi.org/10.1007/BF01010404)
34. N. N. Schraudolph, A fast, compact approximation of the exponential function. *Neural Comput.* **11**, 853–862 (1999). [Medline doi:10.1162/089976699300016467](https://doi.org/10.1162/089976699300016467)